

Simulated Aftershock Sequences for an M 7.8 Earthquake on the Southern San Andreas Fault

Karen Felzer
U.S. Geological Survey

INTRODUCTION

Aftershock activity constitutes one of the largest risks in the aftermath of an earthquake. Aftershocks shake already weakened structures, and if an aftershock is closer to a population center than the original rupture it may cause even more severe local shaking. The 1992 M 6.4 Big Bear aftershock, for example, which occurred several hours after and 40 km to the west of the 1992 M 7.3 Landers, California, mainshock, caused substantially more damage to the city of Big Bear than the Landers earthquake. Even more damaging was the 22 August 1952 M 5.8 Bakersfield, California, aftershock of the M 7.5 Kern County earthquake, which occurred about a month after the mainshock. Due to the proximity of the aftershock to Bakersfield and the weakened condition of the buildings, this aftershock killed two, injured 35, and caused \$10 million in property damage. More recently the 12 May 2008 M 7.9 Sichuan Province, China, earthquake has been followed, as of 1 August 2008, by five aftershocks that caused significant additional injuries, fatalities, and/or major damage.

Given the danger posed by aftershocks it is important to model the type of aftershock sequence that might follow the next large earthquake in southern California. One of the potential large earthquakes that may threaten southern California is an M ~8 on the southern San Andreas fault; a statewide simulation exercise called ShakeOut was held in California in November 2008 to practice response to such a quake. Here I present the 10 different random simulations of the first week of aftershocks that could have accompanied the earthquake modeled for the preparation exercises. Simulation #10 was used for the actual exercises.

No physics is used in the modeling here because aftershock physics are both very complex and controversial. Instead the aftershocks are generated stochastically using established empirical relationships for the distribution of aftershock magnitudes, times, and locations. In addition, each aftershock generates its own aftershocks (secondary aftershocks), an important process that occurs in real sequences (Felzer *et al.* 2003). This type of statistical simulation is known as ETAS (epidemic type aftershock sequences) modeling (Ogata 1998). Only one week of aftershock activity is simulated because we do not expect the simulation exercises to last longer than this and because this will be the most intense period of seismicity. It is important to note,

however, that a mainshock this size is expected to produce aftershocks for years, even decades, and that an aftershock produced at any time may be large (Lomnitz 1966). Thus the long-term aftershock risk should be kept in mind as the simulation exercises are brought to a close.

METHOD

We simulate the aftershocks for the ShakeOut scenario earthquake with the version of the ETAS model developed by Felzer *et al.* (2002), with the addition of an aftershock distribution in space. First we simulate a set of primary, or direct, aftershocks produced by the mainshock over a duration of one week. For this exercise the mainshock is modeled as 22 rectangular sub-faults, each with their own strikes and dips. The aftershocks of the direct aftershocks are then generated, then aftershocks of these aftershocks, etc., until no new earthquakes are produced within the seven-day time period. In order to keep the number of calculations reasonable we only include aftershocks that are at least M 2.5. Earthquakes smaller than this certainly exist and produce aftershocks, but we found that M 2.5 is small enough to make the simulations realistic while keeping the calculations tractable. The parameter values used for the simulation are adjusted for this minimum magnitude.

The aftershock rate as a function of time is given by the modified Omori law (Utsu 1961) expressed in the following form (Reasenber and Jones 1989; Felzer *et al.* 2004),

$$n(t) = k10^{(M_{\text{main}} - M_{\text{min}})}(c + t)^{-p}, \quad (1)$$

where n is the rate of aftershocks larger than or equal to M_{min} , M_{main} is mainshock magnitude, t is time, and k , c , and p are constants. Note that the k , c , and p parameters used for the ETAS model must be for direct aftershock sequences, not for the complete sequences made up of direct plus secondary aftershocks. Our best-fit direct modified Omori law parameters for California are $p = 1.34$, $c = 0.095$ days, and $k = 0.008$, where k is in units of the number of aftershocks $\geq M_{\text{main}}$ produced per day (for details of the parameter solution see Hardebeck *et al.* 2008).

The magnitude of each simulated aftershock is chosen randomly from the Gutenberg-Richter magnitude frequency dis-

tribution, which gives that N , the number of earthquakes larger than or equal to magnitude M , is equal to

$$\log(N) = a - bM \quad (2)$$

(Gutenberg and Richter 1944). Here b is a constant that we set equal to 1.0, and a is a constant that varies with the total number of aftershocks. The law is also truncated for the purposes of the simulation such that no aftershocks larger than M 8 are allowed. Very large aftershocks increase the simulation run time substantially. It should be noted, however, that there is an approximately 4% probability that an M 7.8 mainshock could trigger an $M > 8$ aftershock. Theoretically the largest possible aftershock that could be triggered is equal to the magnitude of the largest possible earthquake that could occur in California.

The distribution of aftershocks in space is modeled using the equation of Felzer and Brodsky (2006), which states that the aftershock density $\rho(r)$ decays with distance from the nearest point on the mainshock fault plane, r , as

$$\rho(r) = cr^{-n}, \quad (3)$$

where $n = 1.37 \pm 0.1$ at 98% confidence for southern California when $\rho(r)$ is given in 1D (linear aftershock density—see Felzer and Brodsky 2006). All $M \geq 5.5$ earthquakes in the simulation are modeled as extended fault planes. The strike of these planes is assigned to be parallel to the strike of the nearest portion of the nearest major California fault. Fault dip is set randomly between 60 deg and 90 deg (reflecting that many southern California faults are strike-slip or thrust), and fault dimensions are taken from the magnitude-area relationships of Wells and Coppersmith (1995). Mainshocks $M < 5.5$ are modeled as point sources. Aftershocks are allowed to be up to 1,000 km away from their mainshock, but are rarely generated at such large distances due to the inverse power law decay of aftershock density. To keep the model simple, extra remotely triggered earthquakes are not assigned to volcanic or geothermal areas, although it has been observed that distant triggering may be more energetic in such regions (Hill *et al.* 1993).

Finally we note that the San Andreas Fault (SAF) scenario mainshock has a unilateral rupture from south to north, and that several studies have shown that triggered earthquakes tend to be more prevalent in the direction of rupture (Gomberg *et al.* 2003). Exactly how much more prevalent, though, is difficult to quantify since there are few well-constrained mainshocks with known unilateral rupture. We roughly infer from inspecting the aftershocks of the fairly unilateral 1992 M 7.3 Landers and 1999 M 7.1 Hector Mine, California, earthquakes that it may be appropriate to place 30% of the aftershocks within 15 degrees of the rupture direction of each fault segment, with the remainder randomly assigned to other azimuths. We do this in our simulations, with the result that a slightly higher portion of aftershocks end up in the SAF Big Bend area and offshore of central and northern California than to the south. Note that this one part of the simulation is rather ad hoc as it is based

on little quantitative data; however, the effect on the earthquake distribution is minimal, simply adding to the aftershock sequence some of the directionality which has been observed in other sequences.

The SAF scenario mainshock also specifies different amounts of slip on the different fault segments, which may be important for aftershock locations. A robust empirical relationship between the amount of slip and the numbers and locations of aftershocks generated has not yet been established, however. So we do not apply any mainshock slip-dependent aftershock density variations here, pending future research.

RESULTS

Not surprisingly, the majority of the aftershocks in all of the sequences occur near the main fault trace. Communities commonly affected by local $M \geq 5.5$ aftershocks include Palm Springs, San Bernardino, Coachella, Wrightwood, Cathedral City, Lancaster, Palmdale, Desert Hot Springs, Mentone, Mecca, and Indio. Looking at some of the larger communities near the fault, six out of the 10 simulations produced one or more $M \geq 5.5$ aftershocks within 20 km of the center of San Bernardino (population 198,000), and five out of the 10 produced one or more such aftershocks within 20 km of the center of Redlands (population 70,000). In addition, all of the scenarios include a minimum of 376 $M \geq 4$ earthquakes in the first week and a minimum of 241 $M \geq 4$ earthquakes on the first day. The main feature of the results, however, is a strong degree of variability between the different sequences. The tamest of our sequences, for example, has only one $M \geq 6$ aftershock in the first week, whereas the most active has 13. The average magnitude of the largest aftershock in each sequence is M 6.9, but the largest aftershock in individual sequences varies from M 6.4 to M 7.7. The total number of $M \geq 5$ aftershocks ranges from 30 to 92, and the total number of $M \geq 3.0$ ranges from 3,812 to 8,380. This variability results from the nonstationary Poissonian process model used to choose the exact timing and magnitude of each aftershock from the empirical statistical distributions (*e.g.*, see Felzer *et al.* 2002) and from the positive feedback of the secondary aftershock triggering process. If a sequence starts out somewhat less active than average, for example, fewer secondary aftershocks will be triggered, resulting in an even lower activity level, whereas a somewhat more active initial sequence or larger than usual aftershock will lead to more and more secondary aftershock generation. Variability is a well-known feature of real aftershock sequences in California; compare the 1990 M_W 5.7 Upland earthquake, for example, with a maximum magnitude aftershock of M 4.72 and 25 $M \geq 3$ aftershocks in the first week with the anemic aftershock sequence of the 1988 M_L 5.02 Pasadena earthquake, which had a maximum magnitude aftershock of M 2.57 and only six $M \geq 2$ earthquakes over the first seven days. Local geology, stress, and variation in mainshock characteristics may account for some of the variation between sequences, but these simulations demonstrate that identical mainshocks and initial parameters can also result in a wide range of aftershock outcomes.

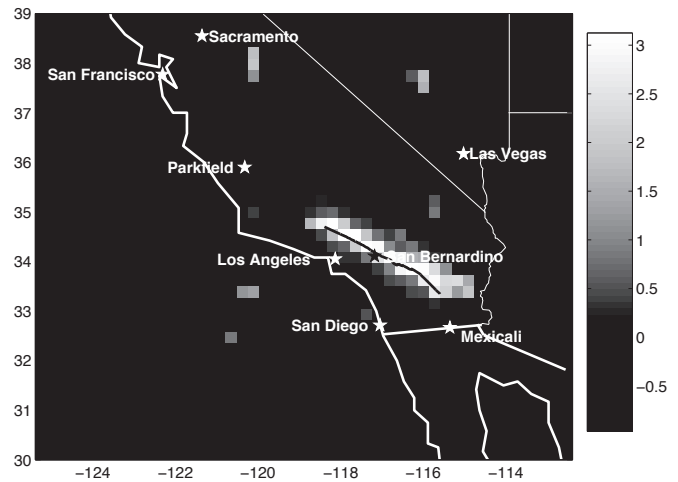
TABLE 1

Summary of the results from the ten aftershock simulations. The first column gives simulation number, the second the largest aftershock produced, the third the day of this largest aftershock (Day 1 is the day of the mainshock), the fourth the total number of $M \geq 5.5$ aftershocks over the seven-day simulation. The final column gives some of the communities expected to be most affected by the largest aftershock.

Sim. #	Largest aftershock	Day of lgst.	No. $M \geq 5.5$	Most Affected Cities
1	6.95	4	20	Sacramento, Modesto, Mariposa
2	6.87	1	9	San Bernardino, Crestline
3	7.09	3	14	Palmdale, Lancaster
4	6.39	1	9	Lancaster
5	6.75	1	21	Wrightwood
6	6.73	1	10	San Bernardino, Yucaipa
7	7.71	4	30	Palm Springs, El Centro
8	6.48	1	13	Little Rock, Lancaster
9	7.28	2	24	Little Rock, Palmdale, Lancaster
10	7.22	1	23	San Gabriel Valley cities

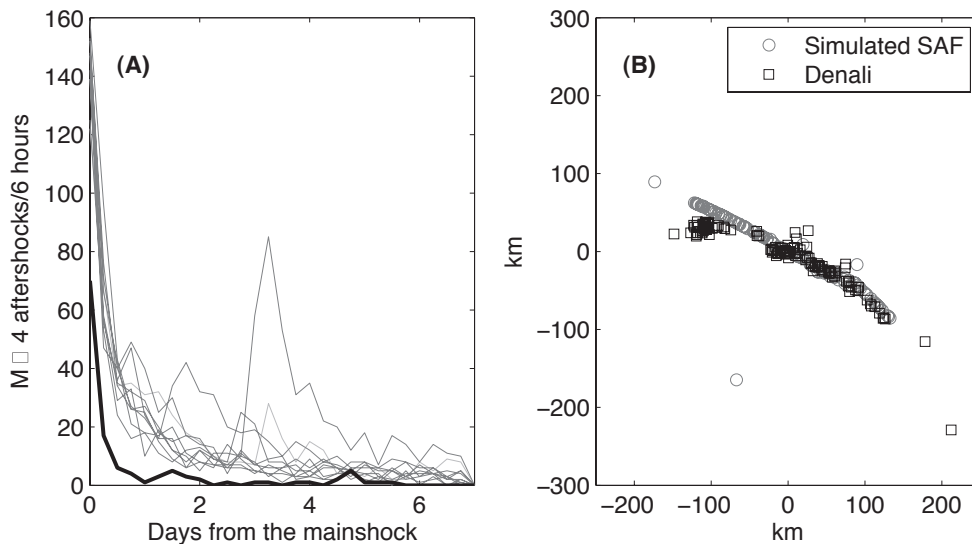
Another important result is that in addition to the clearly significant aftershock risk to communities immediately adjacent to the San Andreas fault, significant aftershocks occasionally happen at greater distances. In one of the simulated scenarios, for example, an M 6.95 occurs east of Sacramento, near the Sierra Nevada, and in another an M 7.2 rips along a parallel trend to the Sierra Madre fault, strongly affecting the San Gabriel Valley, a densely populated region containing over 40 municipalities and about 2 million people. There is clear precedent for such triggering of distant aftershocks by large San Andreas earthquakes; within two days of the 1906 San Francisco San Andreas earthquake, distant aftershocks occurred in or near the Imperial Valley, Pomona Valley, Santa Monica Bay, western Nevada, and western Arizona (Meltzner and Wald 2003); and shortly after the 1857 Ft. Tejon earthquake, additional earthquakes were felt in the northern California cities of Martinez, Benecia, Santa Cruz, San Juan Batista, San Benito, and Mariposa (Townley and Allen 1939). Overall four out of our 10 simulations had one or more $M \geq 5$ aftershocks triggered somewhere north of the central California city of Parkfield. Closer to the mainshock but still removed from the immediate fault trace, half of the simulations produced an $M \geq 6$ earthquake within 50 km of the city of Pasadena, where efforts to collect and catalog earthquake data are centered. None of the simulations produced an $M \geq 6$ within 50 km of the center of Los Angeles, but by extrapolating from the rate of $M \geq 2.5$ occurring in this area we estimate a 1% probability of such an event. A short tabulation of the largest earthquakes in each sequence and the communities most affected is given in Table 1. Average aftershock densities (tabulated in 25×25 -km bins) are mapped in Figure 1.

It is also important to compare our simulated sequences with known aftershock sequences of similar mainshocks. The last major San Andreas fault earthquake to occur in southern California was the 9 January 1857 M 7.9 Ft. Tejon earthquake, which ruptured southward from Parkfield to San Bernardino. A contemporary report, written by a Mr. Barrows for publication in the *San Francisco Bulletin* and marked “Los Angeles, January



▲ **Figure 1.** The logarithm of the average (mean) number of $M \geq 2.5$ aftershocks produced at different locations by the ten simulations. Aftershocks are counted in 25×25 -km bins. The logarithm is used so that regions with both high and low aftershock rates can be seen without saturation of the color map. Bright spots of activity at distant locations from the fault occur where a large aftershock has occurred in a single simulation and produced many secondary aftershocks.

28, 1857,” reported, “We had at Los Angeles five or six shocks during the same day and night and within about eight days time we had twenty shocks—some violent, some light” (Wood 1955). If we assume that all $M \geq 5.5$ shocks along the fault trace would definitely have been felt in Los Angeles, 20 is in the range of the number of such shocks produced in the different simulations (Table 1). Meltzner and Wald (1999), estimating the magnitudes of the aftershocks from historical reports, found M 6.25 and M 6.7 aftershocks in the first eight days occurring near the southern end of the rupture and a later M 6 near San Bernardino and M 6.3 near Parkfield. The simulated scenario 6 came out quite similar to this historic sequence, with one M 6.2



▲ **Figure 2.** This figure provides the time series (rate of aftershocks with time after the mainshock) for the ten simulations and a map of the aftershocks produced in simulation 4. Both the time series and the maps are compared to the first week of aftershocks of the 2002 M 7.9 Denali earthquake, a contemporary earthquake comparable in magnitude and mechanism to the simulated ShakeOut southern San Andreas event. Because the aftershock sequence of the Denali earthquake is complete to $\sim M$ 4 (as estimated from comparison with the Gutenberg-Richter magnitude-frequency relationship [Gutenberg and Richter 1944]), only $M \geq 4$ earthquakes are shown in both plots. (A) Time series of the ten simulated southern SAF aftershock sequences (in gray) and the time series of the first week of the Denali aftershock sequence (in black). Aftershock rate is given as the number of $M \geq 4$ aftershocks measured each quarter day (six hours). Note that the Denali sequence had a very low activity rate in comparison to the worldwide average (see text). For the simulated aftershock sequences, simulation 4 had the fewest aftershocks (376 $M \geq 4$ compared to the 126 detected at Denali), so this simulation is overlain in map view with the first week of $M \geq 4$ Denali aftershocks in (B).

and one M 6.7, both close to the mainshock fault trace, occurring in the first week. The other sequences ranged around this activity rate.

We can also compare our simulation results with the aftershock production from another modern continental strike-slip earthquake, the 2002 M 7.9 Denali earthquake in Alaska, which is perhaps one of the best instrumentally recorded analogs of the simulated ShakeOut southern San Andreas event. The time series and a map view of the simulated aftershocks are compared against the Denali aftershocks in Figure 2. The comparison is hampered, however, by the fact that the local activity of the Denali aftershock sequence was very low—the largest aftershock produced was M 5.8, whereas on average we would normally expect a largest aftershock of $M_{main} - 1.2 = M$ 6.7 (Báth 1965). By chance none of the ten simulations run here came out with a productivity rate this low.

CONCLUSIONS

Our stochastic ETAS simulations indicate that a wide variety of aftershock sequences could accompany the next $M \sim 7.8$ earthquake on the southern San Andreas fault. Some of our ten simulated sequences are similar to the aftershock sequence of the 1857 Ft. Tejon earthquake in terms of a similar number and magnitude of $M \geq 6$ shocks; some are less active, and a few are much more active. One simulation contains an M 7.7 aftershock—nearly as large as the original mainshock. Most simu-

lated large aftershocks affect near-fault communities, with San Bernardino being the largest municipality with a high probability of damaging aftershock activity. One simulation, however, has a distant M 6.95 aftershock located to the east of Sacramento, and another has an M 7.22 along the trend of the Sierra Madre fault, which could be very damaging to a number of San Gabriel Valley communities, including Pomona and Pasadena.

The diversity of the aftershock sequences produced, even though the same mainshock rupture and aftershock production parameters were used for each simulation, results from the randomness of the process and the positive feedback that occurs during secondary aftershock production. Given the inherent variability of the aftershock production process, it is critical to be prepared for the possibility of an active and damaging aftershock sequence after the next Big One—and for the possibility of large aftershocks in unexpected places. ☒

ACKNOWLEDGMENTS

I am grateful to M. Page, E. Pounders, and an anonymous reviewer for thoughtful and thorough reviews and to A. and L. Felzer for editing and assistance. I thank L. Jones and K. Hudnut for inviting me to do the aftershock simulations for the ShakeOut scenario, and I thank K. Hudnut for providing the data for the mainshock rupture planes. Thank you also to everyone who did such hard and quality work for the ShakeOut scenario exercises.

REFERENCES

- Båth, M. (1965). Lateral inhomogeneities in the upper mantle. *Tectonophysics* **2**, 483–514.
- Felzer, K. R., R. E. Abercrombie, and G. Ekström (2003). Secondary aftershocks and their importance for aftershock prediction. *Bulletin of the Seismological Society of America* **93**, 1,433–1,448.
- Felzer, K. R., R. E. Abercrombie, and G. Ekström (2004). A common origin for aftershocks, foreshocks and multiplets. *Bulletin of the Seismological Society of America* **94**, 88–98.
- Felzer, K. R., T. W. Becker, R. E. Abercrombie, G. Ekström, and J. R. Rice (2002). Triggering of the 1999 M_W 7.1 Hector Mine earthquake by aftershocks of the 1992 M_W 7.3 Landers earthquake. *Journal of Geophysical Research* **107**, 2190; doi:10.1029/2001JB000911.
- Felzer, K. R., and E. E. Brodsky (2006). Decay of aftershock density with distance indicates triggering by dynamic stress. *Nature* **441**, 735–738.
- Gomberg, J., P. Bodin, and P. A. Reasenberg (2003). Observing earthquakes triggered in the near field by dynamic deformations. *Bulletin of the Seismological Society of America* **93**, 118–138.
- Gutenberg, B., and C. F. Richter (1944). Frequency of earthquakes in California. *Bulletin of the Seismological Society of America* **4**, 185–188.
- Hardebeck, J. L., K. R. Felzer, and A. J. Michael (2008). Improved test results reveal that the accelerating moment release hypothesis is statistically insignificant. *Journal of Geophysical Research* **113**, B08310; doi:10.1029/2007JB005410.
- Hill, D. P., P. A. Reasenberg, A. Michael, W. J. Arabaz, G. Beroza, D. Brumbaugh, J. N. Brune *et al.* (1993). Seismicity remotely triggered by the magnitude 7.3 Landers, California, earthquake. *Science* **260**, 1,617–1,623.
- Lomnitz, C. (1966). Magnitude stability in earthquake sequences. *Bulletin of the Seismological Society of America* **56**, 247–249.
- Meltzner, A. J., and D. J. Wald (1999). Foreshocks and aftershocks of the great 1857 California earthquake. *Bulletin of the Seismological Society of America* **89**, 1,109–1,120.
- Meltzner, A. J., and D. J. Wald (2003). Aftershocks and triggered events of the Great 1906 California earthquake. *Bulletin of the Seismological Society of America* **93**, 2,160–2,186.
- Ogata, Y. (1998). Space-time point-process models for earthquake occurrences. *Annals of Statistics* **50**, 805–810.
- Reasenberg, P. A., and L. M. Jones (1989). Earthquake hazard after a mainshock in California. *Science* **243**, 1,173–1,176.
- Sornette, A., and D. Sornette (1999). Renormalization of earthquake aftershocks. *Geophysical Research Letters* **26**, 1,981–1,984.
- Townley, S. D., and M. W. Allen (1939). Descriptive catalog of earthquakes of the Pacific Coast of the United States: 1769 to 1928. *Bulletin of the Seismological Society of America* **29**, 1–297.
- Utsu, T. (1961). A statistical study on the occurrence of aftershocks. *Geophysical Magazine* **30**, 521–605.
- Wells, D. L., and K. J. Coppersmith (1995). New empirical relationships among magnitude, rupture length, rupture width, rupture area, and surface displacement. *Bulletin of the Seismological Society of America* **84**, 974–1002.
- Wood, H. O. (1955). The 1857 earthquake in California. *Bulletin of the Seismological Society of America* **45**, 47–68.

*U.S. Geological Survey
525 S. Wilson Avenue
Pasadena, California 91106 U.S.A.
kfelzer@gps.caltech.edu*